Naval Research Laboratory

Washington, DC 20375-5000

NRL Memorandum Report 6087

Electron Energy Deposition in Atomic Nitrogen

R. D. TAYLOR

Berkeley Research Associates
P.O. Box 852
Springfield, VA 22150

S. P. SLINKER AND A. W. ALI

Plasma Theory
Plasma Physics Division

October 6, 1987

A185 H2

SECURITY CLASSIFICATION OF THIS PAGE

REPORT DOCUMENTATION PAGE

Form Approved
OMB No. 0704-0188

1a. REPORT SECURITY CLASSIFICATION UNCLASSIFIED	1b. RESTRICTIVE MARKINGS
2a. SECURITY CLASSIFICATION AUTHORITY	3. DISTRIBUTION / AVAILABILITY OF REPORT Approved for public release; distribution unlimited.
2b. DECLASSIFICATION / DOWNGRADING SCHEDULE	
4. PERFORMING ORGANIZATION REPORT NUMBER(S) NRL-Memorandum Report-6087	5. MONITORING ORGANIZATION REPORT NUMBER(S)
6a. NAME OF PERFORMING ORGANIZATION Naval Research Laboratory 6b. OFFICE SYMBOL (If applicable) Code 4700.1	7a. NAME OF MONITORING ORGANIZATION
6c. ADDRESS (City, State, and ZIP Code) Washington, DC 20375-5000	7b. ADDRESS (City, State, and ZIP Code)
8a. NAME OF FUNDING / SPONSORING ORGANIZATION DARPA 8b. OFFICE SYMBOL (If applicable)	9. PROCUREMENT INSTRUMENT IDENTIFICATION NUMBER
8c. ADDRESS (City, State, and ZIP Code) Arlington, VA 22209	10. SOURCE OF FUNDING NUMBERS PROGRAM ELEMENT NO. 62707E; PROJECT NO. N60921-86-WR-W0233; TASK NO. A63 ARPA Order 4395; WORK UNIT ACCESSION NO. DN680-415
11. TITLE (Include Security Classification) Electron Energy Deposition in Atomic Nitrogen	
12. PERSONAL AUTHOR(S) Taylor,* R.D., Slinker, S.P. and Ali, A.W.	
13a. TYPE OF REPORT Interim 13b. TIME COVERED FROM _____ TO _____	14. DATE OF REPORT (Year, Month, Day) 1987 October 6 15. PAGE COUNT 39
16. SUPPLEMENTARY NOTATION *Berkeley Research Associates, P.O. Box 852, Springfield, VA 22150	

17. COSATI CODES		
FIELD	GROUP	SUB-GROUP

18. SUBJECT TERMS (Continue on reverse if necessary and identify by block number)
Electron energy deposition; Loss function; Nitrogen atom; Cross section

19. ABSTRACT (Continue on reverse if necessary and identify by block number)

A discrete, time-dependent energy deposition model is used to study high-energy electron-beam (100 eV to 10 MeV) deposition in atomic nitrogen. Both time-dependent and steady-state secondary electron distributions are computed. The loss function, mean energies per electron-ion pair production (*DELTA* W), production efficiencies, and yield functions are presented for a wide range of energies. The latest experimental and theoretical cross section are used in the model which predicts ΔW is approximately 31 eV for a wide range of beam energies and background ionization fractions.

delta

20. DISTRIBUTION / AVAILABILITY OF ABSTRACT X UNCLASSIFIED/UNLIMITED ☐ SAME AS RPT. ☐ DTIC USERS	21. ABSTRACT SECURITY CLASSIFICATION UNCLASSIFIED
22a. NAME OF RESPONSIBLE INDIVIDUAL A.W. Ali	22b. TELEPHONE (Include Area Code) (202) 767-3762 22c. OFFICE SYMBOL Code 4700.1

DD Form 1473, JUN 86 *Previous editions are obsolete.* SECURITY CLASSIFICATION OF THIS PAGE

CONTENTS

ELECTRON ENERGY DEPOSITION IN ATOMIC NITROGEN

1. INTRODUCTION

The problem of electron-beam energy deposition in gaseous species is currently of interest in several areas of research, including electron beam propagation in the atmosphere, electron-beam generated lasers, and electron-beam generated discharges and their diagnostics. Detailed deposition calculations generally provide information on the secondary electron distribution, its flux, primary and secondary electron excitation rates for the internal modes of the atoms or molecules, total ionization rate, and the mean energy expended by an electron in generating an electron-ion pair, ΔW. The mean energy, ΔW, is often used to provide a simple description of the cumulative ionization of the gas by high-energy beam electrons, i.e., the creation of secondaries, tertiaries, etc.

In a previous paper[1] (denoted I), we reported on the development of a new electron energy deposition code and its application to the study of deposition in atomic oxygen. While extensive work[1-17] has been done on studying deposition in air and gases such as O, O_2, N_2, H_2, Ar, and He, among others, no such effort has been made for atomic nitrogen. Here, results are presented and discussed for electron-beam energy deposition in atomic nitrogen for beam energies between 100 eV and 10 MeV. Results are obtained using the deposition code mentioned above.[1] In particular, secondary electron distributions are obtained by solving a time-dependent Boltzmann equation. These distribution functions relax to steady-state results from which yield spectra, production efficiencies of specific states, energy partitioning, and ΔW are computed. Loss functions are also computed and compared to Bethe's relativistic equation.[18] Results which are specific to beam deposition in nitrogen are presented. General results are not discussed in detail since the resulting conclusions are identical to those presented in paper I. For example, examinination of $\Phi(T)$ (defined in Eq. (27) in paper I) showed the continuous slowing down approximation (CSDA) to be

Manuscript approved July 24, 1987.

valid for energies greater than 1 keV. Examination of the same quantity for deposition in nitrogen gives the same result and need not be elaborated on further.

The Boltzmann equation and the specific nitrogen model are given in section 2. This includes a discussion of the electron impact excitation and ionization cross sections used in the deposition scheme. The numerical techniques implemented in the calculation were described in detail in the appendix of paper I. Results are presented and discussed in section 3. Summary remarks are reserved for section 4.

2. THE SECONDARY ELECTRON DISTRIBUTION

With the exception of specific nitrogen cross section information, much of the discussion presented in this section was also presented in section 2 of paper I.

The secondary electron distribution for a spatially homogeneous electron beam impinging upon a gas can be calculated from

$$\frac{\partial f}{\partial t}(T,t) = S(T,t) + \sum_s N_s \left\{ \sum_j \left[\sigma_{sj}\left(T+W_{sj}\right) v\left(T+W_{sj}\right) f\left(T+W_{sj},t\right) - \sigma_{sj}(T)\, v(T)\, f(T,t) \right] + \sum_i \left[\int_{T+I_{si}}^{2T+I_{si}} d\varepsilon\, \sigma_{si}\left(\varepsilon,\varepsilon-I_{si}-T\right) v(\varepsilon)\, f(\varepsilon,t) + \int_{2T+I_{si}}^{T_m} d\varepsilon\, \sigma_{si}(\varepsilon,T)\, v(\varepsilon)\, f(\varepsilon,t) - \sigma_{si}(T)\, v(T)\, f(T,t) \right] \right\} + N_p(t) \frac{\partial}{\partial T} \left[L_p(T)\, v(T)\, f(T,t) \right] , \quad (1)$$

where $f(T,t)$ is the secondary electron density ($cm^{-3}\ eV^{-1}$) for electrons with kinetic energy T and speed $v(T)$, $S(T,t)$ the production rate ($cm^{-3}\ sec^{-1}\ eV^{-1}$) due to the incident electron beam, T_m the maximum secondary electron energy (discussed below), N_s the number density of species s, $N_p(t)$ the plasma electron number density, and $L_p(T)$ the loss function of a secondary electron with energy T to the plasma electrons. Loss functions such as $L_p(T)$ are often used to model the effects of electron-electron collisions.[1,2,16,19] The effects of inelastic and ionizing collisions are accounted for by using detailed cross sections. For example, $\sigma_{sj}(T)$ is the j^{th} electron impact excitation cross section for species s where W_{sj} is the excitation energy. For ionization channel i, the total ionization cross section is $\sigma_{si}(T)$, I_{si} the ionization potential, and $\sigma_{si}(\varepsilon,T)$ the (differential) ionization cross section for an incident electron with energy ε producing an additional electron with energy T.

In Eq. (1), electric and magnetic field effects due to the beam are assumed negligible. Elastic and superelastic collisions with the heavy particles are also neglected. Furthermore, in this paper, we consider the case of a single component background gas (atomic nitrogen) and assume that both the gas density ($N_s = N_o$) and source term are time independent. The nitrogen atoms initially reside in the $^4S^o$ (ground) state. The model accounts for energy loss to the $^2D^o$ and $^2P^o$ metastable states, all n = 3 states, 1 specific Rydberg series ($n \geq 4$) state, and the ^3P N^+ state. Within the context of these assumptions and this model, the various terms appearing in Eq. (1) are discussed in detail below. Analytic forms for the relevant excitation and ionization cross sections are presented in sections 2.2 and 2.3. A detailed discussion of these forms, their reduction to well-known theoretical results, and their relative accuracy in comparison to existing measurements and calculations is given elsewhere.[20]

2.1 The Source Term S(T,t)

The emphasis in this paper is on high-energy electron-beam deposition in nitrogen. Beam electrons are assumed to make at most one collision and then leave the area of interest. The source term for the generation of the secondary electrons is, therefore,

$$S(T,t) = S(T) = N_o N_b(T_b) v(T_b) \sum_i \sigma_i(T_b,T) \quad , \qquad (2)$$

where $N_b(T_b)$ is the number density of beam electrons whose energy is T_b, $\sigma_i(T_b,T)$ the differential ionization cross section for producing a secondary electron with energy T (restricted to energies $\leq (T_b - I_i)/2$), and the time-independence is made explicit. The exact form of the differential cross section is discussed in section 2.3.

For the case of energetic electrons which do not leave the area of interest, but are completely stopped by the medium, the source term may be given by

$$S(T,t) = S(T) = N_1 \delta(T - T_b) \quad , \qquad (3)$$

where N_1 is the number of completely stopped electrons per cm^3 per sec. This case is not treated in this paper.

2.2 Electron Impact Excitation Cross Sections

Electron impact excitations of nitrogen are either optically (dipole) allowed or optically forbidden. The cross section for optically allowed transitions from the ground state to an excited state j is given by,

$$\sigma_j = A_j \frac{4\pi a_o^2 R^2 f_j}{E^2} \left(\frac{E}{W_j} - 1 \right) \left\{ \ln \left[\frac{4 C_j E}{W_j} (1 - \beta^2)^{-1} \right] - \beta^2 \right\}, \quad (4)$$

where πa_o^2 is the atomic unit cross section (0.88×10^{-16} cm^2), R the hydrogen atom ionization potential (13.60 eV), W_j the transition energy, f_j the optical oscillator strength, A_j and C_j adjustable parameters, and $\beta = v/c$ where v is the electron velocity. The energy E is $mv^2/2$ where m is the electron rest mass. For energies less than 10^4 eV, E is approximately equal to the electron kinetic energy, T; relativistic effects begin to play a role above that value. All excitation (and ionization) cross sections are assumed equal to 0.0 for energies less than the excitation (or ionization) thresholds. Equation (4) accounts for the threshold behavior in a manner first proposed by Drawin[21] and includes the energy dependence expected according to the relativistic Bethe formula based on the Born approximation.[22,23] It is reasonable to use this form for energies up to 10^9 eV. Above that energy, coupling to the radiation field cannot be neglected.

The parameters used in Eq. (4) for optically allowed transitions are given in Table 1. The oscillator strengths were taken from Wiese et al.[24]

In atomic nitrogen, transitions to forbidden states are categorized as those involving 1) the metastable ground states or 2) higher-lying Rydberg states. Generally, these transitions proceed because of existing electric quadrupole moments, magnetic moments, or electron exchange effects. Cross sections for electron impact excitation of such transitions do not display the characteristic E^{-1} ln E behavior at high energies, but instead decrease more rapidly.[25] To describe such transitions, we adopt a form used extensively by Green and coworkers,[9,26-30]

$$\sigma_j = A_j \frac{4\pi a_o^2 R^2}{(E W_j)^a} \left[1 - \left(\frac{W_j}{E} \right)^b \right]^c , \qquad (5)$$

where a, b, c, and A_j are parameters and the other quantities are defined above. Equation (5), with the proper choice of parameters, reduces to well-known theoretical results.[20]

Table 2 gives the parameters for collisional excitation of the $^2D^o$ and $^2P^o$ metastable states. Two sets of parameters were used to model the metastable state cross sections. These give good agreement with existing experimental[31] and theoretical[32-34] results. Our preference for using two sets of parameters is that the desired E^{-3} high energy behavior[20,21,32] be maintained.

Electron impact excitation cross sections for transitions to high-lying excited states are obtained using the general procedure developed by Green and Dutta.[27] Setting b = 1 and rewriting Eq. (5) to correspond to their form, the cross section is given by,

$$\sigma_j = c_j f_j \frac{4\pi a_o^2 R^2}{W_j^2} \left[1 - \frac{W_j}{E} \right]^c \left(\frac{W_j}{E} \right)^a . \qquad (6)$$

The effective oscillator strength, f_j, is defined as

$$f_j = \frac{f^*}{(n - \rho)^3} , \qquad (7)$$

where ρ and f^* are assumed constant within a Rydberg series and ρ is determined from

$$W_j = I_j - \frac{R}{(n - \rho)^2} . \qquad (8)$$

In principle, the value of f^* is obtained by equating f_j with the known oscillator strength of an optically allowed transition in the series. As an alternative, the parameters c_j, a, c, and ρ may be chosen according to the criteria proposed by Jusick et al.[35] Dalgarno and Lejeune[2] used this method for oxygen, letting f^* vary only according to

which ionization continuum the series belonged to. Adopting their approach, the parameters for all n = 3 states included in this calculation are presented in Table 3. For the ^3P continua, $f^* = 3.475$. We have not included states which ionize to the ^1D or ^1S continua.

Energy loss to Rydberg states with $n \geq 4$ and belonging to a series containing one of the allowed transitions given in Table 1 are also modeled by Eq. (6). The effective f_j is obtained by solving Eq. (8) for ρ (W_j is the energy of the n = 4 state) and integrating Eq. (7) from n = 4 to ∞. $\bar{W}_j$ (the average of W_j and I_j) is used in Eq. (6) in place of W_j. Parameters are given in Table 4.

2.3 Electron Ionization Cross Sections

The total ionization cross section is given, analogous to Eq. (4), by

$$\sigma_i = A_i \frac{4\pi a_o^2 R^2}{E^2} \left(\frac{E}{I_i} - 1 \right) \left\{ \ln \left[\frac{4 C_i E}{I_i} (1 - \beta^2)^{-1} \right] - \beta^2 \right\} \quad . \quad (9)$$

Equation (9) reduces identically to the Drawin formula[21] for low energies, displays the desired $E^{-1} \ln E$ behavior at high energies, and shows the expected rise for relativistic energies.

The differential ionization cross section, $\sigma_i(T,\varepsilon)$, is given by,[13,20]

$$\sigma(T,\varepsilon) = \frac{\sigma(T)}{\tan^{-1}\left[\frac{T-I}{2b(T)}\right]} \frac{b(T)}{b(T)^2 + \varepsilon^2} \quad , \quad (10)$$

for the low energy regime, defined here as $T < I_i + 10$ eV. The index i has been dropped for convenience. When $T > I_i + 10$ eV then

$$\sigma(T,\varepsilon) = \frac{\sigma(T)\, b(T)}{p(T)} g(T,\varepsilon) \quad , \quad (11)$$

where

$$g(T,\varepsilon) = \frac{1}{(T+mc^2)^2} - \frac{(2Tmc^2+m^2c^4)}{(T+mc^2)^2} \frac{1}{(b(T)+\varepsilon)(b(T)+T-\varepsilon-I)}$$

$$+ \frac{1}{b(T)^2 + (T-\varepsilon-I)^2} + \frac{1}{b(T)^2 + \varepsilon^2} \quad , \tag{12}$$

and

$$p(T) = \tan^{-1}\left[\frac{T-I}{b(T)}\right] - \frac{b(T)}{T+2b(T)-I} \frac{(2Tmc^2+m^2c^4)}{(T+mc^2)^2} \ln\left[\frac{b(T)+T-I}{b(T)}\right]$$

$$+ \frac{b(T)(T-I)}{2(T+mc^2)^2} \quad . \tag{13}$$

In Eqs. (10 - 13), b(T) is an energy-dependent parameter and mc^2 the electron rest mass energy (.511 MeV). As above, T is the kinetic energy of the incident electron (primary) and ε the outgoing (secondary) electron. Equation (13) ensures that when the secondary electron is defined as the least energetic of the two, then

$$\sigma_i(T) = \int_0^{(T-I_i)/2} \sigma_i(T,\varepsilon)\, d\varepsilon \quad . \tag{14}$$

The parameters A_i and C_i have been chosen so that Eq. (9) provides a compromise fit to the recent calculations of McGuire[36] and experimental measurements of Brook et al.[37] Additional theoretical and experimental results are discussed in detail elsewhere.[20] Since transitions to $N^+(^1D)$ and $N^+(^1S)$ do not occur in photoionization and, therefore, are expected to have small collision cross sections, they are neglected in this study. The parameter $b_i(T)$ is assumed to have the form

$$b_i(T) = \begin{cases} b_{io} & T \leq \exp(k_i) \\ \dfrac{b_{io}\, k_i}{\ln T} & T \geq \exp(k_i) \end{cases} \quad , \tag{15}$$

where b_{io} and k_i are constants. The ionization parameters are given in Table 5. From the oxygen work,[1] we found that b_{io} is approximately equal to the ionization potential. The functional form of $b_i(T)$ at higher energies and the value of k_i are chosen so that the loss function, L(T), (discussed later below) is in agreement with Bethe's relativistic formula.[18]

2.4 Energy Loss to Plasma Electrons

Perkins[38] has derived the rate of energy loss to plasma electrons by a test electron. These results have been utilized by Schunk and Hayes[19] to obtain expressions for the energy loss for nonrelativistic energies. For relativistic energies, the energy loss is given by Tsytovich.[39] In Eq. (1), these results are used to calculate the loss function, $L_p(T) = -(1/N_p)(dT/dx)$, where

$$-\frac{dT}{dx} = \frac{\omega_p^2 e^2}{v^2} \log \frac{mv^3}{\gamma_o e^2 \omega_p} \quad , \quad kT_e << T << 14.6 \text{ eV} \quad , \qquad (16)$$

$$-\frac{dT}{dx} = \frac{\omega_p^2 e^2}{2v^2} \left\{ \log \frac{mv^2 T}{I_e^2} + 1 - \left[2\left(1-\beta^2\right)^{1/2} + \beta^2 \right] \ln 2 \right.$$

$$\left. + \frac{1}{8} \left[1 - \left(1-\beta^2\right)^{1/2} \right]^2 \right\} \quad , \quad T \geq 14.6 \text{ eV} \quad , \qquad (17)$$

and ω_p is the plasma frequency ($= [4\pi N_p e^2/m]^{1/2}$), $\ln \gamma_o$ is Euler's constant (0.577), T_e the electron temperature, and I_e is an average excitation energy of the plasma electrons given in terms of the dielectric function of the electron gas, $\varepsilon_e(\omega)$, as

$$\ln I_e = \frac{2}{\pi \omega_p^2} \int_0^\infty \omega \, \mathrm{Im} \left[-\varepsilon_e(\omega)^{-1} \right] \ln \hbar\omega \, d\omega \quad . \qquad (18)$$

In the limit of nonrelativistic energies, small damping[36] ($I_e = \hbar\omega_p$), and $N_p << 1.6\times10^{24}$ cm^{-3}, Eq. (17) reduces to the high-energy, nonrelativistic equation given by Perkins.[38] The cutoff energy, 14.6 eV, is chosen to ensure continuity between Eqs. (16 & 17).

In Eq. (1), the ionization fraction, N_p/N_o, is entered as a parameter. For nonrelativistic energies, Dalgarno and Lejeune[2] analyzed the sensitivity of their oxygen deposition model to changes in the fractional ionization. Similar results are presented in the next section.

3. RESULTS

The discrete energy deposition scheme described above and in paper I is utilized for beam electrons with energies ranging from 100 eV to 10 MeV. For all cases, the beam flux was fixed at 1.99×10^{18} cm^{-2} sec^{-1} and the background nitrogen density was fixed at 2.46×10^{19} cm^{-3}. Unless otherwise noted, the fractional ionization was approximately zero (4.1×10^{-20}). The quantities defined below are also defined in paper I. Results for deposition in nitrogen are discussed in this section.

The total inelastic cross section, $\sigma^T(T)$, contains contributions from electron impact excitation, σ_e^T, and ionization, σ_i^T, and is given by,

$$\sigma^T(T) = \sigma_e^T(T) + \sigma_i^T(T)$$

$$= \sum_j \sigma_j(T) + \sum_i \sigma_i(T) \quad . \tag{19}$$

Using the information presented in sections 2.2 and 2.3, these cross sections are shown in Fig. 1 for energies up to 10 MeV.

The loss function accounts for energy loss to excitation, $L_e(T)$, and ionization, $L_i(T)$, as well as energy carried away by secondary electrons, $L_s(T)$, and may be written as

$$L(T) = L_e(T) + L_i(T) + L_s(T)$$

$$= \sum_j W_j \sigma_j(T) + \sum_i I_i \sigma_i(T) + \sum_i \int_0^{(T-I_i)/2} \varepsilon \sigma_i(T,\varepsilon)\, d\varepsilon \quad . \tag{20}$$

Figure 2 shows L(T) and its components for energies up to 10 MeV. Most of the energy goes into producing secondary electrons, while loss to excitation is significant only below the ionization threshold. Figure 2 also shows a comparison between L(T) and Bethe's relativistic loss function,[18]

$$L_B(T) = \frac{2\pi r_e^2 mc^2}{\beta^2} Z \left\{ \log \left[\frac{T^2}{I_o^2} \frac{(\gamma + 1)}{2} \right] + \frac{1}{\gamma^2} - \frac{2\gamma - 1}{\gamma^2} \log 2 \right.$$

$$\left. + \frac{1}{8} \left(\frac{\gamma - 1}{\gamma} \right)^2 \right\} . \qquad (21)$$

In Eq. (21), $Z = 7$ for nitrogen, r_e is the classical electron radius, I_o a mean excitation energy ($I_o = 85.0$ for nitrogen[40]), and $\gamma = (1 - \beta^2)^{-1/2}$. For energies greater than 1 keV, L(T) and $L_B(T)$ are in close agreement. The energy loss of an electron traversing a material is lessened because of polarization of the medium.[40-42] This density effect is small for the energies in the present studies.

Average excitation ($\bar{W}_e$), ionization ($\bar{I}$), and secondary ($\bar{\varepsilon}$) energies (per event) are defined as

$$\bar{W}_e \equiv L_e(T)/\sigma_e^T(T) \quad , \qquad (22)$$

$$\bar{I} \equiv L_i(T)/\sigma_i^T(T) \quad , \qquad (23)$$

$$\bar{\varepsilon} \equiv L_s(T)/\sigma_i^T(T) \quad , \qquad (24)$$

and shown in Fig. 3. There is very little change in $\bar{I}$ and $\bar{W}_e$ for energies greater than ~ 100 eV (asymptotically, $\bar{I} = 14.5$ eV and $\bar{W}_e = 11.9$ eV). The average energy of the secondary electron can be expressed as a function of the incident primary energy, with an accuracy of better than 4%, by

$$\bar{\varepsilon} = 7.93 (\ln T - 2.88) \quad , \quad 100 \text{ eV} \leq T \leq 3 \text{ keV} \quad , \qquad (25)$$

$$\bar{\varepsilon} = 2.75 (\ln T + 6.78) \quad , \quad 3 \text{ keV} \leq T \leq 10 \text{ MeV} \quad . \qquad (26)$$

These averages show that most of the energy in a typical collision goes into producing secondaries.

The CSDA is valid for energies greater than approximately 1 keV. Within this approximation, total excited state and ion populations after degradation of the primary may be calculated using the ratios $\sigma_e^T(T)/L(T)$ and $\sigma_i^T(T)/L(T)$. These quantities are shown in Fig. 4.

The time-dependent Boltzmann equation was solved using numerical methods discussed in the appendix of paper I. In general, the distribution function, f(T,t), relaxes to a steady-state solution, f(T). For a 10 MeV beam, this relaxation is shown in Fig. 5. The characteristic relaxation time is energy-dependent. Intermediate energies (~ 100 eV) relax first, followed by the lower part of the spectrum (~ 10 eV, but greater than the lowest excitation energy), and, finally, the high energies ($\gtrsim$ 1 keV). Similar observations were made by Bretagne et al.[15] for Ar and in paper I for oxygen. Figure 6 shows steady-state distribution functions for various beam energies.

Yield spectra, Y(T), [$= N_o \sigma^T(T) v(T) f(T)$] are shown in Fig. 8. These are proportional to similar quantities analyzed by Green and coworkers.[10-12] For completely stopped source electrons (from 50 eV to 10 keV), Green et al.[12] find that the yield functions fall off with energy as $T^{-1.58}$. Our oxygen results[1] show that this energy dependence holds for beam sources as well. For nitrogen, the energy behavior of the yield spectra are also independent of source energy. This result was also found by Garvey et al.[10,11] for H_2 and beam energies up to 10 MeV.

As mentioned previously, the energy necessary to produce an electron-ion pair, ΔW, is particularly useful for simplifying the description of ionization in a gas. For beam sources, it is given by

$$\Delta W = \frac{N_o \, N_b(T_b) \, v(T_b) \, L(T_b)}{\int S(T) \, dT + \sum_i N_o \int \sigma_i(T) \, v(T) \, f(T,t) \, dT} , \qquad (29)$$

where the first term in the denominator gives the rate for producing electron-ion pairs directly by beam ionization and the second term is the production rate for all generations of secondaries. Equation (29)

shows that ΔW is, in general, a time-dependent function, through its dependence on $f(T,t)$. The steady-state values of ΔW for beam energies ranging from 100 eV to 10 MeV are shown in Table 6. These values are nearly constant (to within 2%) over the entire energy range. The near constancy of ΔW at energies $\gtrsim$ 100 eV is well-known.[10,43,44] Fano[44] attributes this result to the fact that the ratios of the excitation and ionization cross sections are insensitive to energy. Garvey et al.[10] use the independence of the yield spectra on source energy to give an analytic demonstration of this effect.

For a given state, the production efficiency, $P_j(T_b)$, is defined as the number of excitations of that state per electron-ion pair created, i.e.,

$$P_j(T_b) = \frac{N_o \int \sigma_j(T)\, v(T)\, f(T,t)\, dT}{N_o\, N_b(T_b)\, v(T_b)\, L(T_b) / \Delta W} \quad . \tag{29}$$

For a 10 MeV beam, the six largest production efficiencies are given in Table 7. These production efficiencies are nearly constant for beam energies of 100 eV to 10 MeV. The production efficiency for the single ionization continuum is unity.

The results discussed above depend, in part, on the value of the assumed ionization fraction.[2] The sensitivity of these results has been investigated. In particular, Fig. 8 shows that the distribution function, $f(T)$, is insensitive to changes in the background ionization for energies greater than $\sim$ 20 eV, but highly sensitive for lower energies. Table 8 shows ΔW and the percentage of deposition energy lost to the background electrons for various ionization fractions. As expected, the energy loss increases with increasing numbers of background electrons, however, ΔW remains nearly constant until the fraction approaches 10^{-2}.

4. SUMMARY

A discrete model has been used to study energy deposition by relativistic electron beams in atomic nitrogen. For beam energies between 100 eV and 10 MeV, the energy required to produce an electron-ion pair is approximately 31 eV. For a 10 MeV beam, ΔW is also constant for background ionization fractions between 0.0 and 10^{-3}. Production efficiencies remain nearly constant over most of the energy range. The time-dependent model is used to observe the relaxation of the secondary electron distribution to a steady state solution. These are the first results for deposition in atomic nitrogen.

ACKNOWLEDGEMENT

This work was supported by the Defense Advanced Research Projects Agency under ARPA Order No.4395, Amendment No. 63, and monitored by the Naval Surface Weapons Center.

REFERENCES

1. S.P. Slinker, R.D. Taylor, and A.W. Ali, "Electron Energy Deposition in Atomic Oxygen" (submitted to J. Appl. Phys.).

2. A. Dalgarno and G. Lejeune, Planet. Space Sci. 19, 1653 (1971).

3. A.E.S. Green and C.A. Barth, J. Geophys. Res. 70, 1083 (1965).

4. A.E.S. Green and C.A. Barth, J. Geophys. Res. 72, 3975 (1967).

5. R.S. Stolarski and A.E.S. Green, J. Geophys. Res. 72, 3967 (1967).

6. L.R Peterson, Phys. Rev. 187, 105 (1969).

7. S.D. Rockwood, Phys. Rev. A8, 2348 (1973).

8. S.D. Rockwood, J.E. Brau, W.A. Proctor, and G.H. Caravan, IEEE J. Quantum Electron. 9, 120 (1973).

9. H.S. Porter, C.H. Jackman, and A.E.S. Green, J. Chem. Phys. 65, 154 (1976).

10. R.H. Garvey, H.S. Porter, and A.E.S. Green, J. Appl. Phys. 48, 4353 (1977).

11. R.H. Garvey, H.S. Porter, and A.E.S. Green, J. Appl. Phys. 48, 190 (1977).

12. A.E.S. Green, C.H. Jackman, and R.H. Garvey, J. Geophys. Res. 82, 5104 (1977).

13. Y.A. Medvedev and V.D. Khokhlov, Sov. Phys. Tech. Phys. 24, 181 (1979); ibid 185 (1979).

14. P.S. Ganas and A.E.S. Green, J. Quant. Spectrosc. Radiat. Transfer 25, 265 (1981).

15. J. Bretagne, G. Delouya, J. Godart, and V. Puech, J. Phys. D14, 1225 (1981).

16. D.J. Strickland and A.W. Ali, "A Code for the Secondary Electron Energy Distribution in Air and Some Applications", NRL Memorandum Report 4956, Washington, D.C. (1982).

17. S. Slinker and A.W. Ali, "Electron Energy Deposition in Atomic Oxygen", NRL Memorandum Report 5909, Washington, D.C. (1986).

18. H.A. Bethe, Handbuch der Physik, Vol. 24, p. 273, Springer, Berlin (1933).

19. R.W. Schunk and P.B. Hayes, Planet. Space Sci. 19, 113 (1971).

20. R.D. Taylor and A.W. Ali, "Excitation and Ionization Cross Sections for Electron-Beam Energy Deposition in High Temperature Air", NRL Memorandum Report xxxx, Washington, D.C. (1987). Also, R.D. Taylor and A.W. Ali (to be published).

21. H.W. Dravin, "Collision and Transport Cross Sections", Report EUR-CEA-FC-383, Fontenay-aux-Roses (1966) and revised (1967).

22. H. Bethe, Z. Physik 76, 293 (1932).

23. For an excellent discussion of the Bethe theory for inelastic collisions of fast charged particles with atoms see, M. Inokuti, Rev. Mod. Phys. 43, 297 (1971) and M. Inokuti, Y. Itikawa, and J. Turner, Rev. Mod. Phys. 50, 23 (1978).

24. W.L. Wiese, M.W. Smith, and B.M. Glennon, "Atomic Transition Probabilities", NSRDS-NBS4, vol. 1, U.S. Government Printing Office, Washington, D.C. (1966).

25. N.F. Mott and H.S.W. Massey, The Theory of Atomic Collisions (3rd edition) Clarendon Press, Oxford (1965).

26. L.R. Peterson, S.S. Prasad, and A.E.S. Green, Can. J. Chem. 47, 1774 (1969).

27. A.E.S. Green and S.K. Dutta, J. Geophys. Res. 72, 3933 (1967).

28. A.E.S. Green and R.S. Stolarski, J. Atmos. Terr. Phys. 34, 1703 (1972).

29. A.E.S. Green and T. Savada, J. Atmos. Terr. Phys. 34, 1719 (1972).

30. C.H. Jackman, R.H. Garvey, and A.E.S. Green, J. Geophys. Res. 82, 5081 (1977).

31. R.H. Neynaber, LL. Marino, E.W. Rothe, and S.M. Trujillo, Phys. Rev. 129, 2069 (1963).

32. R.J.W. Henry, P.G. Burke, and A.-L. Sinfailam, Phys. Rev. 178, 218 (1969).

33. S. Ormonde, K. Smith, B.W. Torres, and A.R. Davies, Phys. Rev. A8, 262 (1973).

34. K.A. Berrington, P.G. Burke, and W.D. Robb, J. Phys. B8, 2500 (1975).

35. A.T. Jusick, C.E. Watson, L.R. Peterson, and A.E.S. Green, J. Geophys. Res. 72, 3943 (1967).

36. E.J. McGuire, Phys. Rev. A3, 267 (1971).

37. E. Brook, M.F. Harrison, and A.C.H. Smith, J. Phys. B11, 3115 (1978).

38. F. Perkins, Physics of Fluids 8, 1361 (1965).

39. V.N. Tsytovich, Zh. Eksp. Teor. Fiz. 42, 803 (1962) [Sov. JETP 15, 561 (1962)]; R.J. Gould, Physica (Utr.) 60, 145 (1972); L. Vriens, Phys. Rev. A8 332 (1973).

40. L. Pages, E. Bertel, H. Joffre, and L. Sklavenitis, At. Data 4, 1 (1972).

41. E. Fermi, Phys. Rev. 57, 485 (1940).

42. R.M. Sternheimer, Phys. Rev. 145, 247 (1966).

43. A. Dalgarno, in Atomic and Molecular Processes (Edited by D.R. Bates) Academic Press, New York (1962).

44. U. Fano, Phys. Rev. 70, 44 (1946).

Table 1

Electron Impact Excitation Cross Section Parameters
for Optically Allowed Transitions

State	W_j	A_j	C_j	f_j
^4P 3s	10.33	1.0	0.3125	0.130
^4P $2s2p^4$	10.92	1.0	0.3125	0.350

Table 2

Electron Impact Excitation Cross Section Parameters
for Metastable-State Transitions

State	W_j	A_j	a	b	c	
$^2D^o$ $2p^3$	2.38	0.025	1	1	1	$\leq$ 40.0 eV
		227.72	3			$\geq$ 40.0 eV
$^2P^o$ $2p^3$	3.57	0.0175	1	1	1	$\leq$ 40.0 eV
		356.04	3			$\geq$ 40.0 eV

Table 3

Electron Impact Excitation Cross Section Parameters
for Rydberg-State Transitions

State	W_j	c_j	f_j	a	c
^2P 3p	10.68	0.40	0.150	2	1
$^2S^o$ 3p	11.60	0.30	0.191	2	1
$^4D^o$ 3p	11.75	0.10	0.130	1	1
$^4P^o$ 3p	11.84	1.50	0.130	0.7	2.5
$^4S^o$ 3p	11.99	0.07	0.150	0.7	0.5
$^2D^o$ 3p	12.00	0.14	0.140	2	1
$^2P^o$ 3p	12.12	0.40	0.150	2	1
^2D 3s'	12.35	--	--	-	-
^2P 3d	12.97	0.40	0.150	2	1
^4F 3d	12.98	0.10	0.130	1	1
^2F 3d	12.99	0.14	0.140	2	1

Table 3 (continued)

State	W_j	c_j	f_j	a	c
^4P 3d	12.99	1.50	0.130	0.7	2.5
^4D 3d	13.01	0.10	0.130	1	1
^2D 3d	13.03	0.14	0.140	2	1
$^2D^o$ 3p'	13.70	--	--	-	-
$^2F^o$ 3p'	13.72	--	--	-	-
$^2P^o$ 3p'	13.92	--	--	-	-
^2S 3s''	14.41	--	--	-	-
^2G 3d'	14.89	--	--	-	-
^2S 3d'	14.94	--	--	-	-

Table 4

Electron Impact Excitation Cross Section Parameters
for Rydberg Series ($n \geq 4$) Transitions

State	$\bar{W}_j$	C_j	f_j	a	c
^4P ns	13.70	1.50	0.109	0.7	2.5

Table 5

Electron Impact Ionization Cross Section Parameters

Final State	A_i	C_i	b_{io}	k_i
$N^+(^3P)$	2.20	0.25	15.0	7.40

Table 6

ΔW Versus Electron Beam Energy, T_b

T_b (eV)	10^2	10^3	10^4	10^5	10^6	10^7
ΔW (eV)	30.9	30.8	31.0	31.4	31.4	30.8

Table 7

Production Efficiencies for a 10 MeV Beam

State	P_j	State	P_j
$^2D^o$ $2p^3$	1.55	^4P 3p	0.13
$^2P^o$ $2p^3$	0.35	^4P 3d	0.11
^4P 3s	0.32		
^4P $2s2p^4$	0.14	$N^+(^3P)$	1.0

Table 8

ΔW and Energy Loss Versus Ionization Fraction

Fraction	0.0	10^{-6}	10^{-5}	10^{-4}	10^{-3}	10^{-2}
ΔW (eV)	30.8	30.8	30.8	30.8	30.9	31.8
Energy Loss (%)	0.0	3.5	4.0	5.9	11.9	22.0

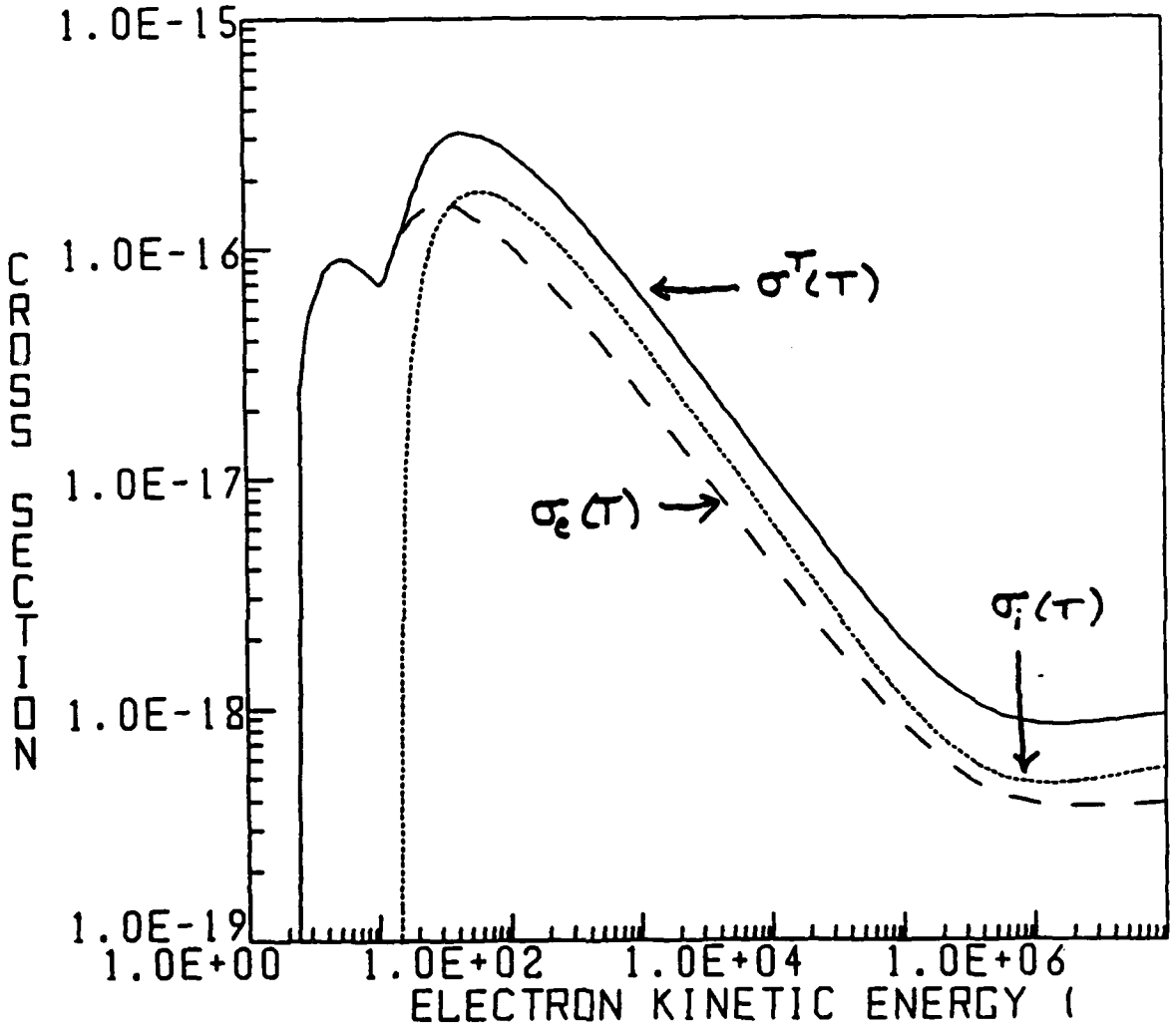

Fig. 1. Total excitation (long dashes), total ionization (short dashes), and total inelastic (solid line) cross sections.

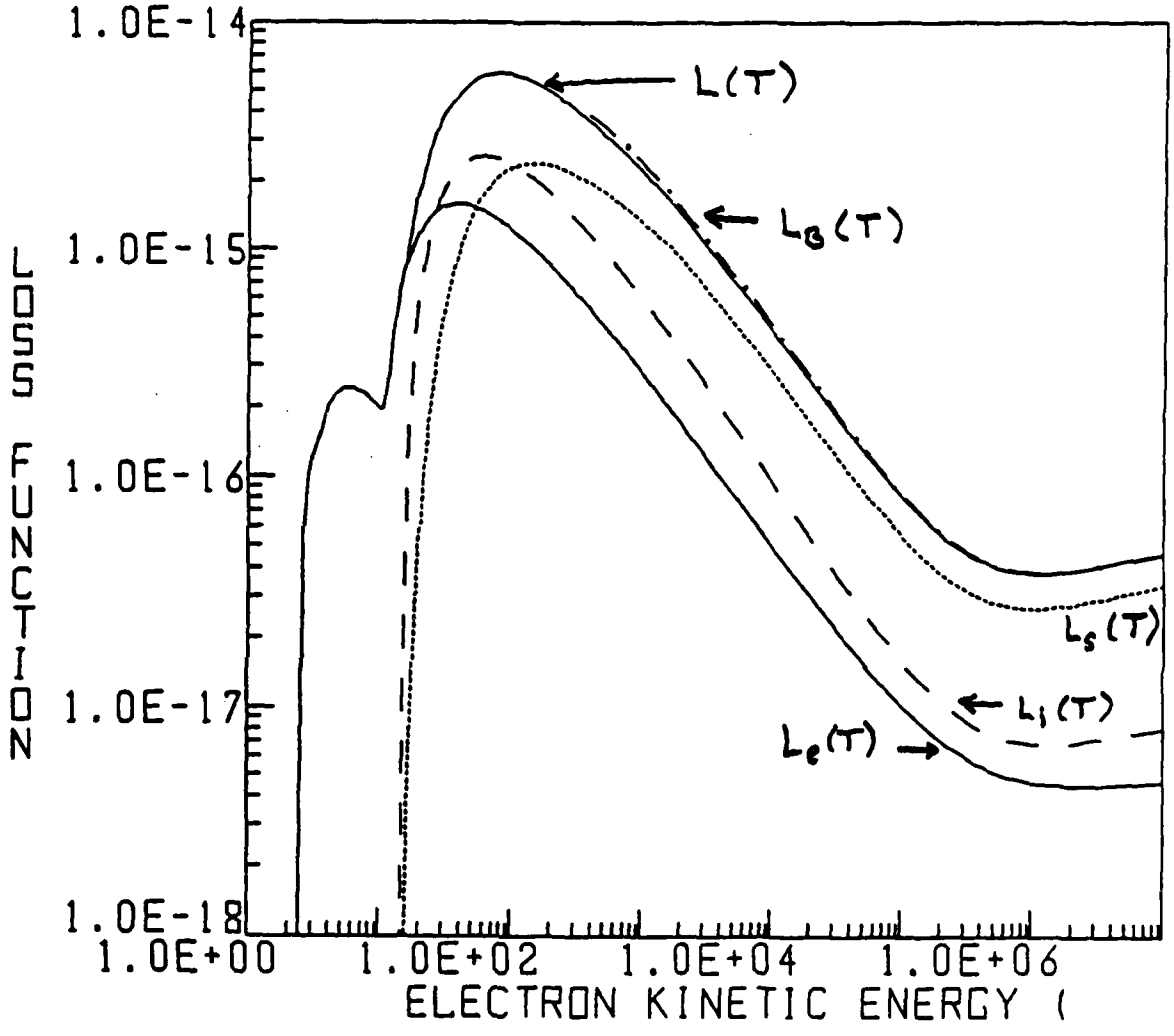

Fig. 2. Total loss function (solid line) partitioned into excitation (lower solid line), ionization (long dashes), and secondary electron (short dashes) contributions and compared to Bethe's formula, Eq. (21) (dash-dotted line).

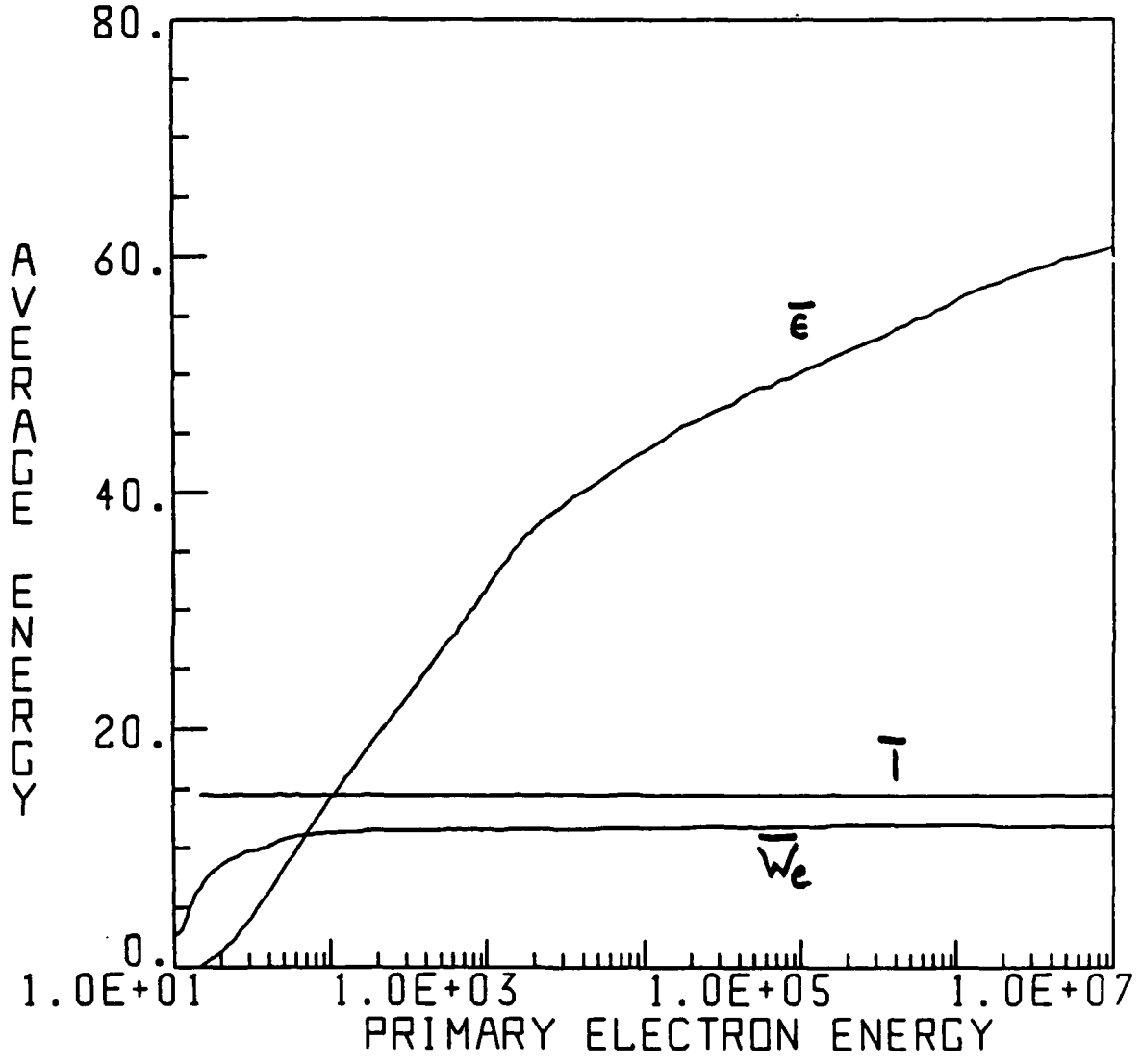

Fig. 3. Average excitation, ionization, and secondary energies defined according to Eqs. (22 - 24).

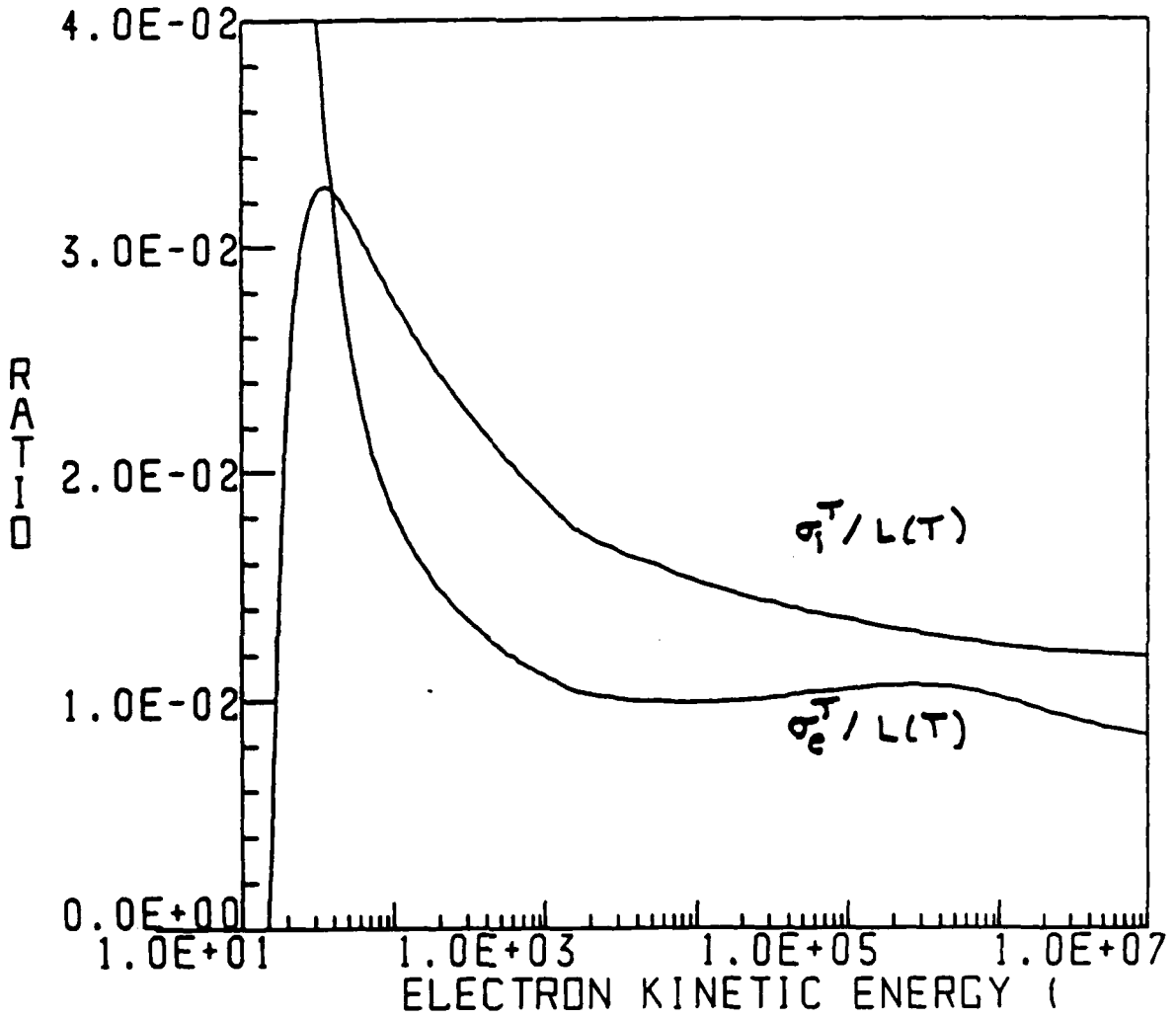

Fig. 4. Ratio of the total excitation and ionization cross sections to the total loss function.

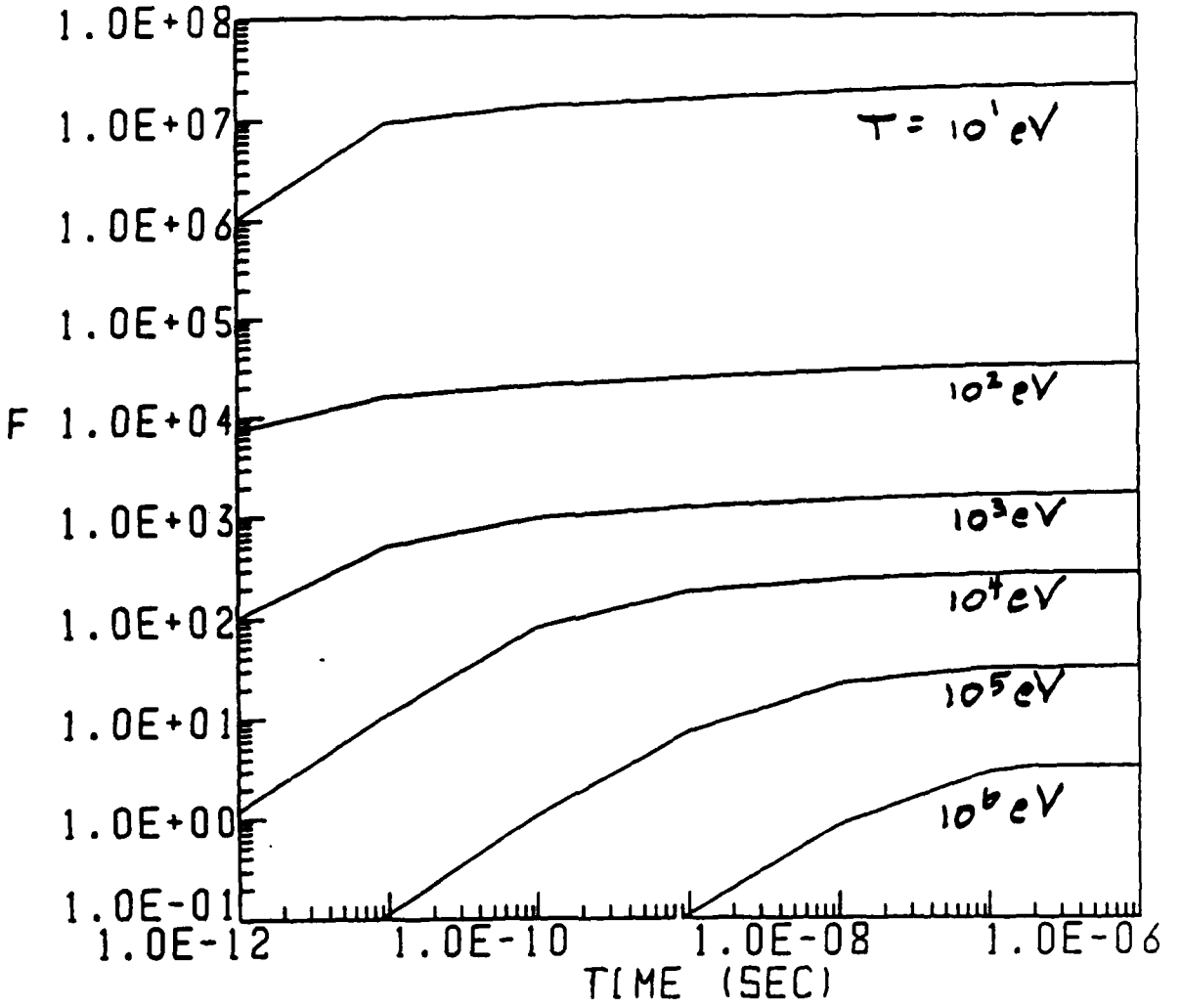

Fig. 5. Relaxation of f(T,t) to steady-state for T = 10^1 - 10^6 eV.

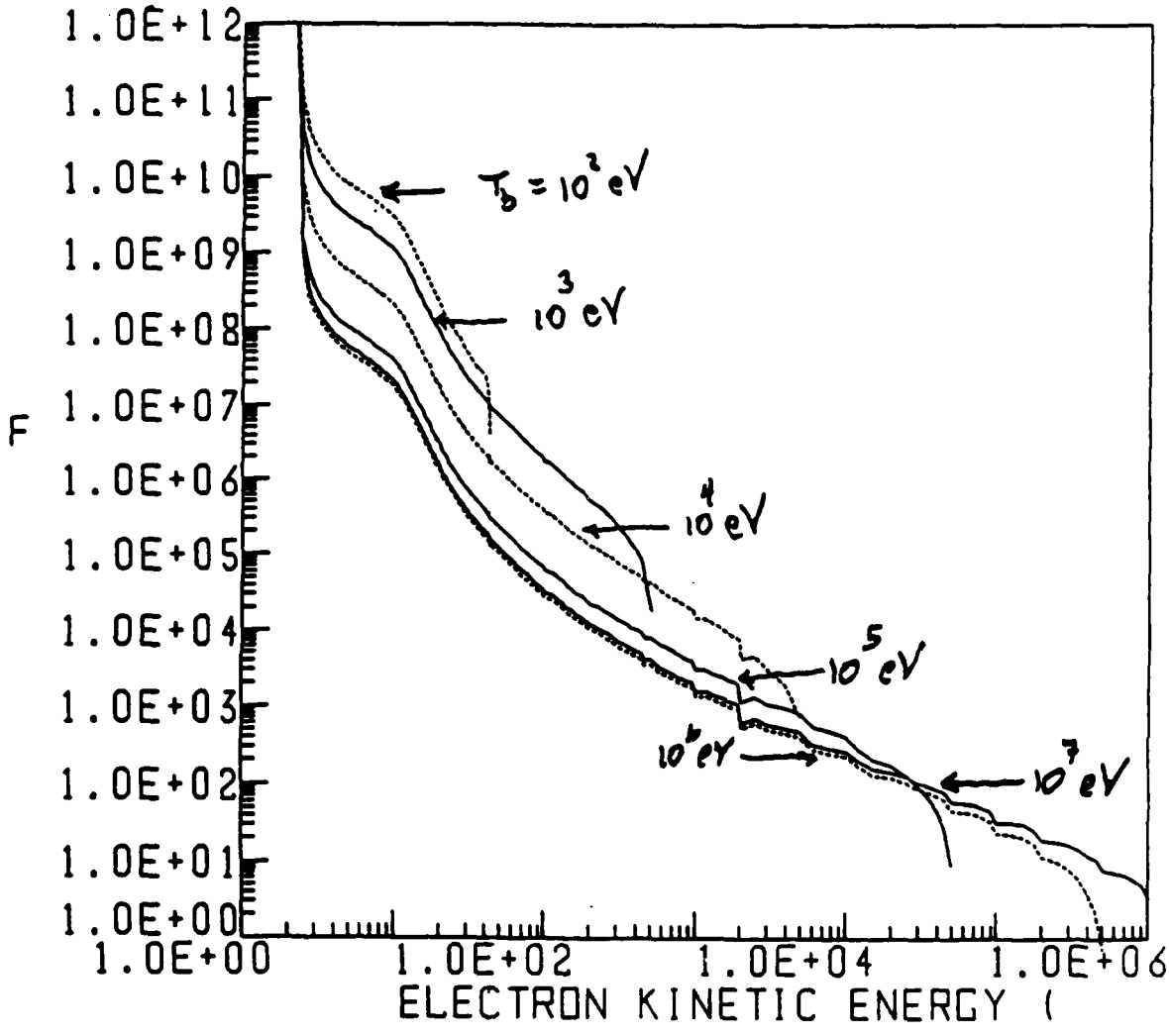

Fig. 6. Steady-state distribution function, f(T), for beam energies of 100 eV to 10 MeV.

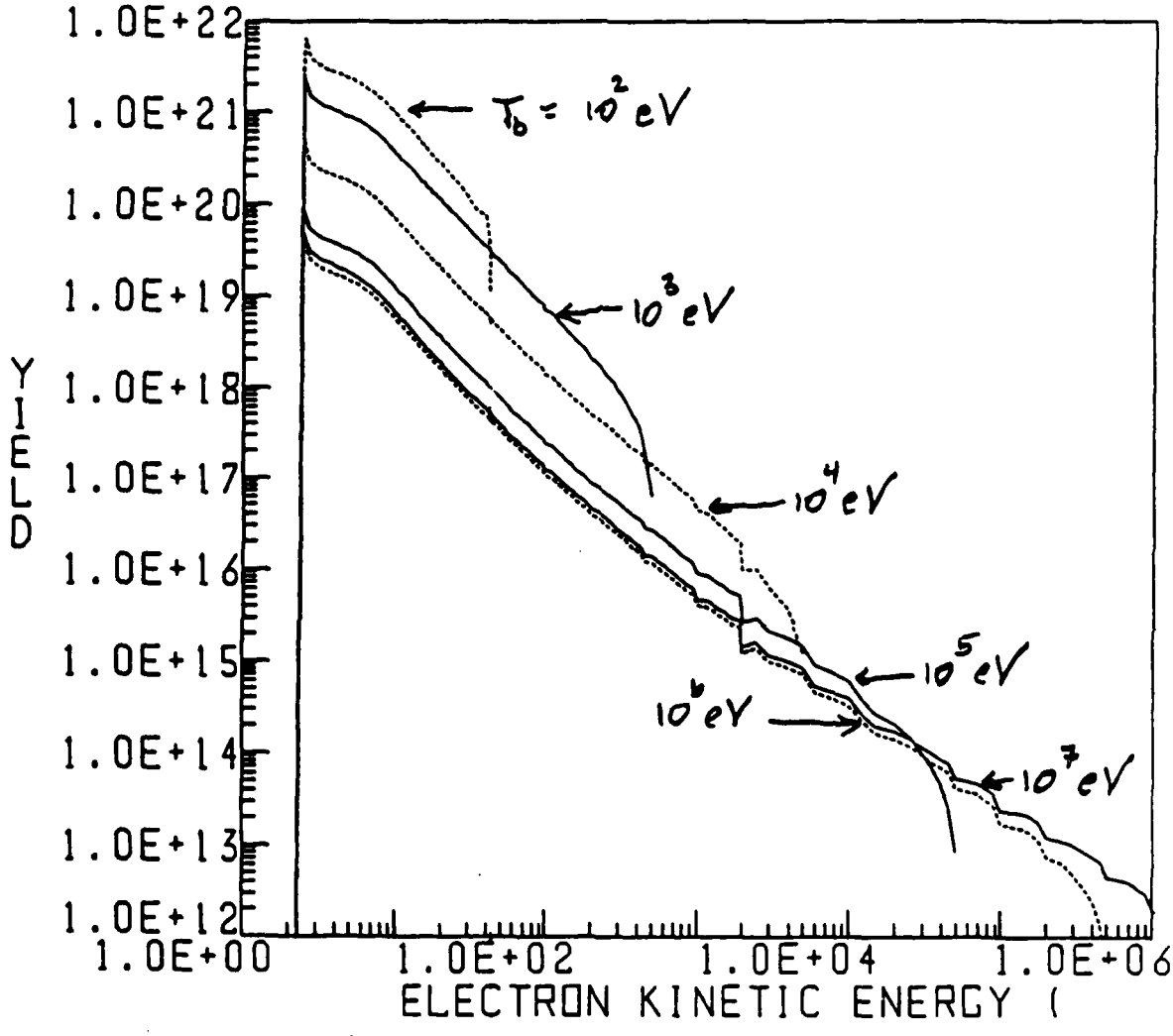

Fig. 7. Yield spectra for beam energies of 100 eV to 10 MeV.

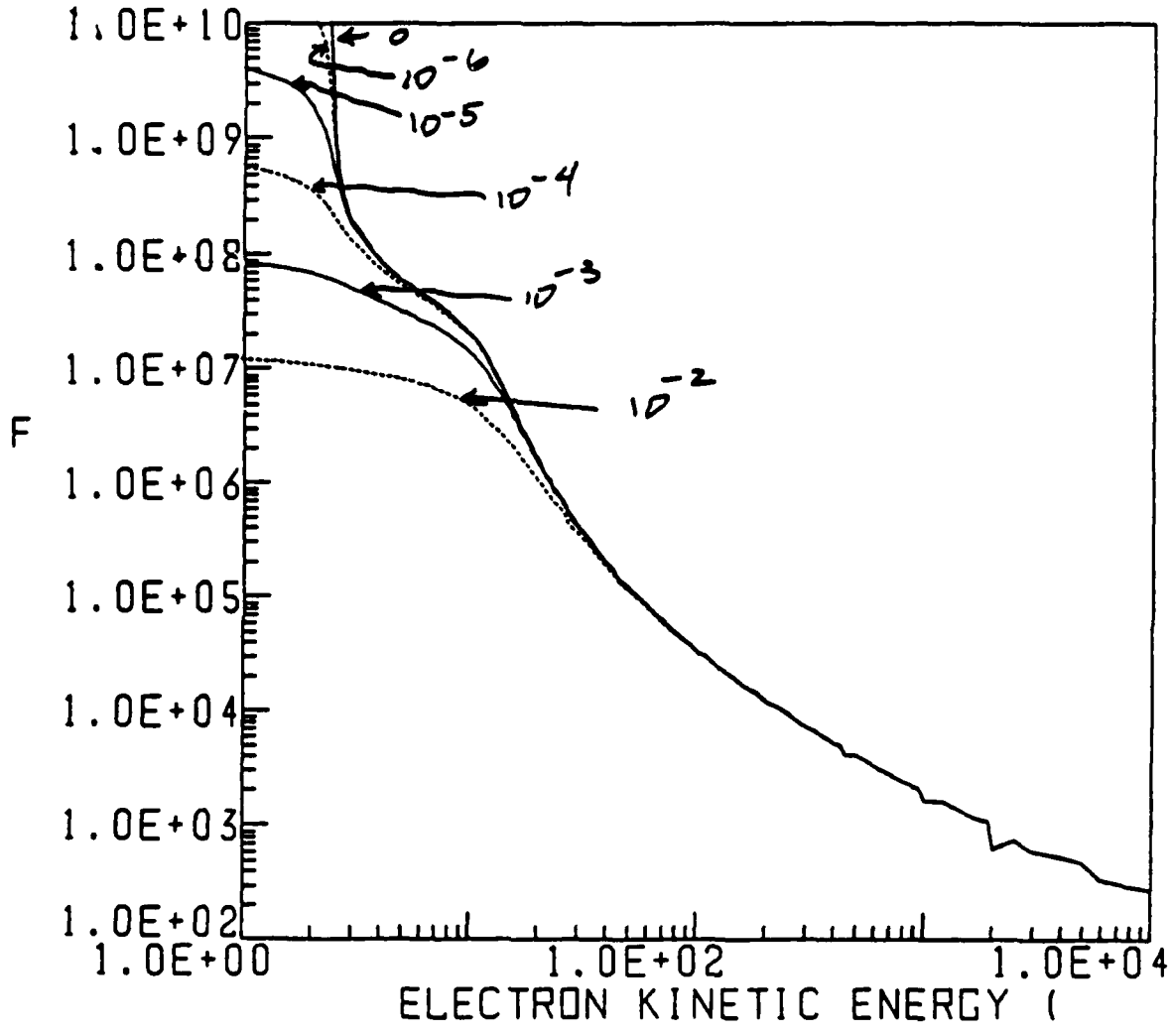

Fig. 8. f(T) for fractional ionizations of 0 - 10^{-2}.

Distribution List

Naval Research Laboratory
4555 Overlook Avenue, S.W.
Washington, D.C. 20375-5000
Attn: Dr. M. Lampe - Code 4792 (2 copies)
Dr. T. Coffey - Code 1001
Dr. J. Boris - Code 4040
Dr. M. Picone - Code 4040
Dr. J. B. Aviles - Code 4665
Dr. M. Haftel - Code 4665
Dr. S. Ossakow - Code 4700 (26 copies)
Dr. A. Ali - Code 4700.1 (30 copies)
Dr. M. Friedman - Code 4700.1
Dr. R. Taylor - BRA (4700.1)
Mr. I. M. Vitkovitsky - Code 4701
Dr. S. Gold - Code 4740
Dr. A. Robson - Code 4760
Dr. M. Raleigh - Code 4760
Dr. R. Meger - Code 4763
Dr. D. Murphy - Code 4763
Dr. R. Pechacek - Code 4763
Dr. G. Cooperstein - Code 4770
Dr. D. Colombant - Code 4790
Dr. R. Fernsler - Code 4790
Dr. I. Haber - Code 4790
Dr. R. F. Hubbard - Code 4790
Dr. G. Joyce - Code 4790
Dr. Y. Lau - Code 4790
Dr. S. P. Slinker - Code 4790
Dr. P. Sprangle - Code 4790
Code 4790 (20 copies)
Library - Code 2628 ~~(20~~ 22 copies)
D. Wilbanks - Code 2634
Code 1220

Air Force Office of Scientific Research
Physical and Geophysical Sciences
Bolling Air Force Base
Washington, DC 20332
Attn: Major Bruce Smith

Air Force Weapons Laboratory
Kirtland Air Force Base
Albuquerque, NM 87117
Attn:
W. Baker (AFWL/NTYP)
D. Dietz (AFWL/NTYP)
Lt Col J. Head

U. S. Army Ballistics Research Laboratory
Aberdeen Proving Ground, Maryland 21005
Attn: Dr. Donald Eccleshall (DRXBR-BM)
Dr. Anand Prakash

Avco Everett Research Laboratory
2385 Revere Beach Pkwy
Everett, Massachusetts 02149
Attn: Dr. R. Patrick
Dr. Dennis Reilly

Ballistic Missile Def. Ad. Tech. Ctr.
P.O. Box 1500
Huntsville, Alabama 35807
Attn: Dr. M. Hawie (BMDSATC-1)

Chief of Naval Material
Office of Naval Technology
MAT-0712, Room 503
800 North Quincy Street
Arlington, VA 22217
Attn: Dr. Eli Zimet

Cornell University
Ithaca, NY 14853
Attn: Prof. David Hammer

DASIAC - DETIR
Kaman Tempo
25600 Huntington Avenue, Suite 500
Alexandria, VA 22303
Attn: Mr. F. Wimenitz

Defense Advanced Research Projects Agency
1400 Wilson Blvd.
Arlington, VA 22209
Attn: Dr. Shen Shey
Dr. H. L. Buchanan

Defense Technical Information Center
Cameron Station
5010 Duke Street
Alexandria, VA 22314 (2 copies)

Department of Energy
Washington, DC 20545
Attn: Dr. Terry F. Godlove (ER20:GTN,
High Energy and Nuclear Physics
Mr. Gerald J. Peters (G-256)

Directed Technologies, Inc.
226 Potomac School Road
McLean, VA 22101
Attn: Dr. Ira F. Kuhn
Dr. Nancy Chesser

C. S. Draper Laboratories
555 Technology Square
Cambridge, Massachusetts 02139
Attn: Dr. E. Olsson
Dr. L. Matson

Institute for Fusion Studies
University of Texas at Austin
RLM 11.218
Austin, TX 78712
Attn: Prof. Marshall N. Rosenbluth

Intelcom Rad Tech.
P.O. Box 81087
San Diego, California 92138
Attn: Dr. W. Selph

Joint Institute for Laboratory
Astrophysics
National Bureau of Standards and
University of Colorado
Boulder, CO 80309
Attn: Dr. Arthur V. Phelps

Kaman Sciences
1500 Garden of the Gods Road
Colorado Springs, CO 80933
Attn: Dr. John P. Jackson

Lawrence Berkeley Laboratory
University of California
Berkeley, CA 94720
Attn: Dr. Edward P. Lee

Lawrence Livermore National Laboratory
University of California
Livermore, California 94550
Attn: Dr. Richard J. Briggs
Dr. Simon S. Yu
Dr. Frank Chambers
Dr. James W.-K. Mark, L-477
Dr. William Fawley
Dr. William Barletta
Dr. William Sharp
Dr. Daniel S. Prono
Dr. John K. Boyd
Dr. Kenneth W. Struve
Dr. John Clark
Dr. George J. Caporaso
Dr. William E. Martin
Dr. Donald Prosnitz

Lockheed Palo Alto Laboratory
3251 Hanover St.
Bldg. 203, Dept 52-11
Palo Alto, CA 94304
Attn: Dr. John Siambis

Los Alamos National Scientific Laboratory
P.O. Box 1663
Los Alamos, NM 87545
Attn: Dr. L. Thode
Dr. M. A. Mostrom, MS-608
Dr. H. Dogliani, MS-5000
Dr. R. Carlson
Ms. Leah Baker, MS-P940
Dr. Carl Ekdahl

Maxwell Laboratories Inc.
8888 Balboa Avenue
San Diego, CA 92123
Attn: Dr. Ken Whitham

McDonnell Douglas Research Laboratories
Dept. 223, Bldg. 33, Level 45
Box 516
St. Louis, MO 63166
Attn: Dr. Evan Rose
Dr. Carl Leader

Mission Research Corporation
EM Systems Applications
1720 Randolph Road, S.E.
Albuquerque, NM 87106
Attn: Dr. Brendan Godfrey
Dr. Thomas Hughes
Dr. Lawrence Wright
Dr. A. B. Newberger

Mission Research Corporation
P. O. Drawer 719
Santa Barbara, California 93102
Attn: Dr. C. Longmire
Dr. N. Carron

National Bureau of Standards
Gaithersburg, Maryland 20760
Attn: Dr. Mark Wilson

Naval Surface Weapons Center
White Oak Laboratory
Silver Spring, Maryland 20903-5000
Attn: Dr. R. Cawley
Dr. J. W. Forbes
Dr. E. E. Nolting
Mr. W. M. Hinckley
Mr. N. E. Scofield
Dr. E. C. Whitman
Dr. M. H. Cha
Dr. H. S. Uhm
Dr. R. Fiorito
Dr. K. T. Nguyen
Dr. R. Stark
Dr. R. Chen

Office of Naval Research
800 North Quincy Street
Arlington, VA 22217
Attn: Dr. C. W. Roberson
Dr. W. S. Condell (Code 421)

Office of Under Secretary of Defense
Research and Engineering
Room 3E1034
The Pentagon
Washington, DC 20301
Attn: Mr. John M. Bachkosky

ORI, Inc.
1375 Piccard Drive
Rockville, MD 20850
Attn: Dr. C. M. Huddleston

Physical Dynamics, Inc.
P.O. Box 1883
La Jolla, California 92038
Attn: Dr. K. Brueckner

Physics International, Inc.
2700 Merced Street
San Leandro, CA. 94577
Attn: Dr. E. Goldman

Princeton University
Plasma Physics Laboratory
Princeton, NJ 08540
Attn: Dr. Francis Perkins, Jr.

Pulse Sciences, Inc.
14796 Wicks Blvd.
San Leandro, CA 94577
Attn: Dr. Sidney Putnam
Dr. John Bayless

Sandia National Laboratory
Albuquerque, NM 87115
Attn: Dr. Bruce Miller
Dr. Barbara Epstein
Dr. John Freeman
Dr. Gordon T. Leifeste
Dr. Gerald N. Hays
Dr. James Chang
Dr. Michael G. Mazerakis
Dr. John Wagner
Dr. Ron Lipinski

Science Applications Intl. Corp.
5150 El Camino Real
Suite B31
Los Altos, CA 94022

Attn: Dr. R.R. Johnston
Dr. Leon Feinstein
Dr. Douglas Keeley

Science Applications Intl. Corp.
1710 Goodridge Drive
McLean, VA 22102
Attn: Mr. W. Chadsey
Dr. A Drobot
Dr. K. Papadopoulos
Dr. B. Hui

Commander
Space & Naval Warfare Systems Command
PMW-145
Washington, DC 20363-5100
Attn: CAPT J. D. Fontana
CDR W. Bassett

SRI International
PSO-15
Molecular Physics Laboratory
333 Ravenswood Avenue
Menlo Park, CA 94025
Attn: Dr. Donald Eckstrom

Strategic Defense Initiative Org.
1717 H Street, N. W.
Washington, DC 20009
Attn: Lt Col R. L. Cullickson
Dr. J. Ionson
Dr. D. Duston

Strategic Defense Initiative Office
Directed Energy Weapons Office, The Pentagon
Office of the Secretary of Defense
Washington, DC 20301-7100
Attn: Dr. C. F. Sharn (OP0987B)

Titan Systems, Inc.
9191 Towne Centre Drive, Suite 500
San Diego, CA 92122
Attn: Dr. R. M. Dowe

University of California
Physics Department
Irvine, CA 92664
Attn: Dr. Gregory Benford
University of Maryland
Physics Department
College Park, MD 20742
Attn: Dr. Y. C. Lee
Dr. C. Grebogi

University of Michigan
Dept. of Nuclear Engineering
Ann Arbor, MI 48109
Attn: Prof. Terry Kammash
Prof. R. Gilgenbach

Director of Research
U.S. Naval Academy
Annapolis, MD 21402 (2copies)